

RSC Advances



This is an *Accepted Manuscript*, which has been through the Royal Society of Chemistry peer review process and has been accepted for publication.

Accepted Manuscripts are published online shortly after acceptance, before technical editing, formatting and proof reading. Using this free service, authors can make their results available to the community, in citable form, before we publish the edited article. This *Accepted Manuscript* will be replaced by the edited, formatted and paginated article as soon as this is available.

You can find more information about *Accepted Manuscripts* in the [Information for Authors](#).

Please note that technical editing may introduce minor changes to the text and/or graphics, which may alter content. The journal's standard [Terms & Conditions](#) and the [Ethical guidelines](#) still apply. In no event shall the Royal Society of Chemistry be held responsible for any errors or omissions in this *Accepted Manuscript* or any consequences arising from the use of any information it contains.



Journal Name

ARTICLE

Multi-Functional Fluorescent Scaffold as a Multi-colour Probe: Design and Application in Targeted Cell Imaging

M. Kesik,^a B. Demir,^b F. B. Barlas,^b C. Geyik,^c S. C. Cevher,^a D. Odaci Demirkol,^b S. Timur,^{*,b,c} A. Cirpan,^{a,d} and L. Toppare^{*,a,d,e}

Received 00th January 20xx,
Accepted 00th January 20xx

DOI: 10.1039/x0xx00000x

www.rsc.org/

A novel scaffold material based on a novel targeting strategy has been developed, benefiting from recent progress in development of fluorescent bioprobes. This concept suggests that several specifications which are desired for cancer cell targeting and imaging studies can be satisfied at the same time in one multifunctional scaffold. Besides, such scaffold exhibits multi-colour properties when combined with a targeting moiety. For this purpose, a fluorescent and functional monomer, 3-(1H-phenanthro[9,10-d]imidazol-2-yl)phenol (PIP) and an antibody labelling kit (CF555) were merged on the same scaffold to generate the proposed bioprobe. This design offers multicolour cell images by emitting at dual wavelengths with no quenching in its fluorescent property. Also, pendant alcohol groups in the structure of PIP enable covalent attachment to labelled protein; CF555/anti-CD44 in order to enhance the biological activity and specificity towards the target. After combining with targeting moiety, the bioconjugate was characterized, tested for *in vitro* studies, and the cellular internalization was monitored in live cells via fluorescence microscope technique. The present work with such strategy explores the potential use of the proposed fluorescent probe for the first time. The aim is to achieve targeted imaging of CD44 positive U87-MG cancer cells and determine specific cellular labelling via fluorescence imaging and flow cytometry experiments.

1. Introduction

Great attention has been paid to the design and development of novel fluorescent probes due to their potential applications in the field of biomedicine since fluorescence based strategies are of great interest in understanding cellular and physiological processes and probing biomolecular interactions.¹⁻³ Also, the use of fluorescent probes has become a promising approach for more efficient diagnosis of wide spread threat; cancer. This type of materials should be highly fluorescent, photostable, available for bioconjugation, have good biocompatibility, maximum spatial resolution, and minimal perturbation to biological systems.⁴ To date, various organic and inorganic molecules like fluorescent organic dyes, nanomaterials and conjugated polymers were used for cancer cell targeting and imaging purposes.⁵ Most of the existing fluorescent materials designed exhibit superior characteristics yet together with important disadvantages. Thus, scientists like our group have

developed new fluorescent materials with improved properties to enhance targeting and imaging ability.⁶⁻⁸

Yagci et al⁸ developed a fluorescent probe combining single walled carbon nanotubes (SWCNT) with a copolymer; (PPP-*g*-PSt-PCL) which contains poly(para-phenylene) (PPP), polystyrene (PSt) and poly(ϵ -caprolactone) (PCL) side chains. In that study the polymer was non-covalently bound to carboxyl functional SWCNTs. Folic acid conjugation of the probe was achieved for targeted imaging of folate receptor (FR) overexpressing cancer cells. *In vitro* studies show that this conjugate can specifically bind to HeLa cells. Liu and coworkers⁹ developed anti-HER2-conjugated multifunctional nanoparticles (MFNPs) with a core-shell structure of UCNP@Fe₃O₄@Au using the layer-by-layer assembling system. It was presented that these bioconjugated MFNPs can detect breast cancer BT474 cells (HER2+). Jana et al¹⁰ synthesized Europium incorporated ZnO-chemically converted graphene nanocomposites. Fluorescence images of MCF7 cancer cells with the nanocomposite indicate the internalization of the nanomaterials within the cells.

These studies are just few examples in this field. When one focused on the studies of developing fluorescent probes for cancer cell targeting and imaging, we figured out that regardless of the material type, a number of particular drawbacks were observed.^{11,12} This has motivated us to search for a totally new strategy for the development of fluorescent probes for effective targeting and imaging. Developing new strategies can have remarkable effect on the effort of the

^a Department of Chemistry, Middle East Technical University, 06800 Ankara, Turkey

^b Department of Biochemistry, Faculty of Science, Ege University, 35100 Bornova-Izmir, Turkey

^c Institute on Drug Abuse, Toxicology and Pharmaceutical Science, Ege University, 35100 Bornova-Izmir, Turkey

^d The Center for Solar Energy Research and Applications (GUNAM), Middle East Technical University, 06800 Ankara, Turkey

^e Department of Biotechnology, Middle East Technical University, 06800 Ankara, Turkey

perfect fluorescent marker design. By this way, scientists can focus on specifically success of the targeting cell imaging. Accordingly, the newly proposed fluorescence probe behaves as a multifunctional scaffold for the cellular imaging system. Such scaffold would exhibit multicolour properties when combined with a targeting moiety. The ideal design has to satisfy several requirements. (1) It should emit at two different wavelengths in order to achieve multicolour cell images. (2) These emission wavelengths should be significantly different to avoid quenching in their fluorescence property. (3) The composition can be tuned according to desired functionality. (4) The fluorescent probe, for sure, should mimic some of essential properties like photostability and biocompatibility. Thus, it is possible to detect cellular internalization in live cells precisely without any necessity of overcoming all the drawbacks. In other words, such scaffold system provides self-checking of the system. By this way, scientists can change their mind in the design of perfect fluorescent markers for targeting cell imaging purpose. However, the major challenge in this type of system is to combine all these requirements in one scaffold. Hence, achieving this goal requires the incorporation of multiple materials such as an organic fluorophore, a dye or a nanomaterial on the targeted probe which exhibit their own benefits on the same platform.

Wang et al¹³ described such a multicolour system which was prepared using a conjugated polymer nanoparticle (CPN) together with four different polymers having different emissions. They used carboxyl functionalized CPNs prepared by a co-precipitation method based on hydrophobic interactions between the conjugated polymers and poly(styrene-co-maleic anhydride) (PSMA). The resulting properties were influenced by changing the choice, amount and ratio of CPN. However, in this design, polymers were in co-precipitated form and their conjugation backbones were present in the same solution. In other words, emission characteristics of the polymers can affect each other since they exist in the same conjugation path length. In the present design such an effect is minimized. The presence of anti-CD44, due to its structural nature, behaves as a non-conjugated spacer. Thus, the target bioconjugate consisting of different structures will exhibit independent emission characteristics in one scaffold.

Herein, we report a fluorescent probe which satisfies all the requirements mentioned above in order to examine cell specific binding ability of the bioconjugate. We selected a functional and fluorescent monomer; 3-(1H-phenanthro[9,10-d]imidazol-2-yl)phenol (PIP) and a commercial organic dye (CF555). Biomolecule conjugation was performed with anti-CD44 and specific cellular labelling was determined by fluorescence imaging and flow cytometry experiments. The monomer PIP was synthesized and used as the part of the proposed scaffold. Pendant alcohol groups in the structure of the monomer enable covalent attachment to targeting moiety, anti-CD44. Such modification enhances the biological activity and specificity towards the target.¹⁴ Moreover, it can be excited at 350 nm exhibiting blue fluorescence. Also, CF555 is an antibody labelling kit which labels the antibody. The dye,

excited at 555 nm, is covalently linked to the antibody to exhibit red fluorescence. After labelling the anti-CD44 biomolecule, the monomer was linked to the labelled antibody through covalent binding using well-known carbonyldiimidazole (CDI) chemistry.¹⁵ The resulting bioconjugate was used as the fluorescent probe, which can be emitted at two different wavelengths for targeted imaging of CD44 positive U87-MG cancer cells. Furthermore, the covalent attachment of the monomer PIP to the labelled anti-CD44 preserves its fluorescence character after bioconjugation. Hence targeting of cancer cells was achieved with no significant quenching in fluorescence. The bioconjugate was tested for in vitro studies, and the cellular internalization was monitored in live cells via fluorescence microscope technique. Expression of the CD44 receptor in U87-MG cells and HaCaT control cells was confirmed by flow cytometry. The results present that this strategy enables the bioconjugate to specifically bind U87-MG cells with high efficiency. To our best knowledge, this work represents the first demonstration of this type of fluorescent probe design. The key advances of this system are ability to synthesize the scaffold according to desired functions and use as an efficient fluorescent probe for cell targeting and imaging. Hence, such a probe design can shed new light into the biomedical sensing and diagnosis technologies.

2. Materials and Methods

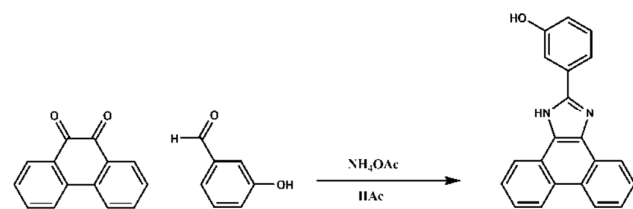
Reagents and Materials

9,10-phenanthrenequinone, 3-hydroxybenzaldehyde, ammonium acetate (NH₄OAc), Mix-n-Stain CF555 antibody labelling kit and carbonyldiimidazole (CDI) were purchased from Sigma Aldrich (St. Louis, USA; www.sigmaaldrich.com) and acetic acid was purchased from Merck (Darmstadt, Germany; www.merck.com). Anti-CD44 antibody (ab41478) was purchased from Abcam. Reactions were performed under ambient atmospheric conditions. All solvents were analytical grade. Other inorganic and organic materials were commercially available and used as received.

Dulbecco's modified Eagle Medium (DMEM), Eagle's Minimum Essential Medium (EMEM), Fetal bovine serum (FBS), penicillin/streptomycin (P/S) (10000/10000 units) and 200 mM L-Glutamine were purchased from Lonza. U87-MG (neuroglioma cells, ATCC) and HaCaT (Human keratinocytes, CLS) cell lines were maintained in EMEM and DMEM, respectively. Both of them supplemented with 10.0% FBS, and 1.0% P/S at 37°C in a humidified incubator with 5.0% CO₂ in air. All cells were sub-cultured at 80% confluency by trypsinization every two or three days.

Measurements and Characterizations

¹H NMR (400 MHz) and ¹³C NMR (100 MHz) spectra were recorded on a Bruker Spectrospin Avance DPX-400 MHz spectrometer using deuterated dimethyl sulfoxide (DMSO) as the solvent and tetramethylsilane (TMS) as the internal



reference. Fluorescence measurements of conjugates were accomplished with a VarioskanTMFlash Multimode Reader

Scheme 1. Synthesis of 3-(1H-phenanthro[9,10-d]imidazol-2-yl)phenol (PIP).

(Thermo Scientific, USA). Atomic force microscopy (AFM) to study modified surfaces were carried out on Veeco Multimode V AS-130 ("J"). The tapping mode was used to take topographic images. Plasma oxygen-treated silicon wafer as the substrate was used for measurements. Samples were prepared *via* drop-coating.

Synthesis of 3-(1H-phenanthro[9,10-d]imidazol-2-yl)phenol (PIP)

10 mmol 9,10-phenanthrenequinone (2.08 g), 10 mmol 3-hydroxybenzaldehyde (1.22 g) 40 mmol NH_4OAc (3.08 g) were dissolved in 60 mL acetic acid. After refluxing for 12 h, solution was cooled and poured into ice water. Precipitates were collected and washed copiously with water and 150 mL methanol. Resulting off-white precipitates (2.26 g, 7.3 mmol) were used without further purification (%73). Scheme 1 shows the reagents and conditions of the reaction.

^1H NMR (DMSO): δ 13.25 - 13.70 (br, NH), δ 9.75 (s, OH), δ 8.86 (d, 2H, J = 8.2 Hz, δ 8.57 (d, 2H, J = 7.7 Hz), δ 7.70 - 7.78 (m, 4H), δ 7.64 (dd, 2H, J^1 = 7.4 Hz J^2 = 7.3 Hz), δ 7.40 (dd, 1H, J^1 = 7.8 Hz, J^2 = 7.7 Hz), δ 6.91 (dd, 1H, J^1 = 8.2 Hz J^2 = 1.6 Hz).

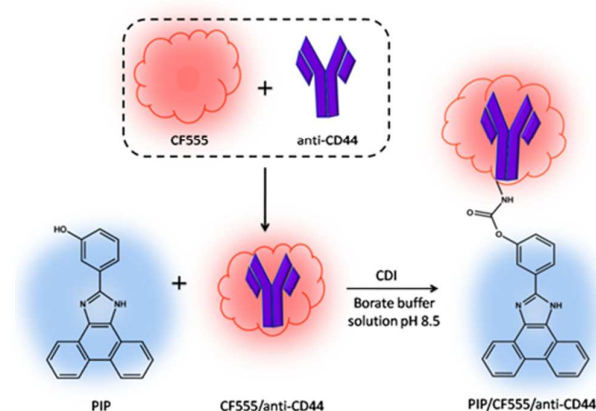
^{13}C NMR (DMSO): δ 157.7, 149.2, 131.4, 129.9, 127.5, 127.1, 125.3, 123.8, 121.9, 117.0, 116.4, 113.0.

Synthesis of the bioconjugate

1.0 mg PIP and 10 mg CDI were dissolved in 200 μL DMSO. The solution was incubated for 2 h at 37°C with 1000 rpm to activate pendant alcohol groups of PIP for further coupling with antibody. The solution was diluted with 400 μL DMSO and 900 μL borate buffer solution (50 mM, pH 8.5). At the same time, CF555 dye was attached covalently to the anti-CD44 antibody via following the protocol. Then, 8.0 μL of labelled antibody solution and 200 μL of activated PIP with CDI solution were mixed in 42 μL borate buffer solution (50 mM, pH 8.5) to obtain target concentration of 20 $\mu\text{g}/\text{mL}$ labelled antibody and 400 $\mu\text{g}/\text{mL}$ activated PIP with CDI solution. It was shaken for 4 h at room temperature with 1000 rpm. Unconjugated biomolecules, excess reagents were separated via centrifugation with distilled water using 10 kDa membrane filters. For the all-cell culture experiments and characterizations, only freshly prepared conjugates were used. Scheme 2 depicts the construction procedure of the proposed bioconjugate for PIP/CF555/anti-CD44.

Cell Viability

A cell proliferation assay kit (MTT reagent) was used to determine the changes in cell viability of cells treated with samples. To perform the MTT assay, both U87-MG cells and HaCaT cells were seeded into 96 well plates and incubated until reaching confluency with normal morphology. The samples of PIP monomer, PIP/anti-CD44 and PIP/CF555/anti-CD44 with concentrations of 1.0, 2.0, 4.0, 10, 20, 40, 100 and 200 $\mu\text{g}/\text{mL}$ were added to wells and then the cell culture plates were placed into CO_2 incubator for incubation at 37°C for 2 h. After incubation the cells were washed to remove culture medium. MTT assay on the cell lines was carried out according to standard procedure.¹⁶ The dose-dependent cytotoxicity of bioconjugates was reported as cell viabilities relative to the control (untreated) cells.



Scheme 2. Preparation of PIP/CF555/anti-CD44 bioconjugate.

Flow Cytometry Analysis

To compare CD44 expression levels, U87-MG and HaCaT cells were stained with anti-CD44 antibody (Sigma) and anti-rabbit IgG (H+L) Alexa Fluor[®] 488 (Invitrogen). For cell staining, cells were harvested and washed with cold PBS. Additional washing step was performed with incubation buffer (2.0% FBS in PBS). Pellet was treated with incubation buffer and maintained to obtain 1.0×10^6 cells per assay. After centrifugation, cell pellet was incubated with 2.0 μg anti-CD44 antibody in 500 μL incubation buffer for 1 h at room temperature. Negative control staining was performed without primary antibody (e.g. 500 μL incubation buffer). Unbound antibodies were removed by washing the cells three times in incubation buffer before adding secondary antibody. Samples were incubated with Anti-rabbit IgG (H+L) Alexa Fluor[®] 488 (1:2000 in incubation buffer) for 45 min at ambient conditions. Unbound antibodies were removed by washing the cells three times with incubation buffer. 10,000 cells were analyzed in BD FACS flow cytometer for Alexa Fluor[®] 488 signals. Data were plotted as fluorescence intensity/count histograms using FlowJo software (Tree Star, San Carlos, CA). Normalized median fluorescence intensity

(nMFI) was calculated from median fluorescence intensity (MFI) values of histograms using the following equation:

$$nMFI = \frac{(MFI_{CD44} / MFI_{Control})_{U87-MG}}{(MFI_{CD44} / MFI_{Control})_{HaCaT}} \quad (\text{Eq. 1})$$

Fluorescence Microscopy - Cell Culture Experiments

In order to observe the interactions of the prepared conjugates with both U87-MG and HaCaT cells, 100 μL of samples (20 $\mu\text{g}/\text{mL}$) were introduced into the cells grown in a chamber slide for two days. The cell images were taken via fluorescence microscope (Olympus BX53F) equipped with a CCD camera (Olympus DP72). After treatment for 2 h at 37 $^{\circ}\text{C}$ in CO_2 incubator, the cells were washed twice with PBS. Cell photographs were given separately according to the structure of bioconjugates and excitation fields.

3. Results and Discussion

Characterizations of PIP/CF555/anti-CD44 bioconjugate

Our strategy for design and synthesis of fluorescence probe is to combine different requirements in one scaffold. While the blue fluorescent monomer PIP serves as a strong candidate for covalent attachment to the anti-CD44 using well-known CDI chemistry, CF555 dye has a strong emission in the red region of visible spectrum which can be linked covalently to the protein. The target bioconjugate was tested for in vitro studies, and the cellular internalization was monitored in CD44 positive U87-MG cancer cells via fluorescence microscope technique. The designed bioconjugate were prepared using PIP and CF555 linked anti-CD44 in different ratios to overcome nonspecific binding of the protein and to get maximum solubility in water. From a synthetic point of view, the strategy describes a new approach for design and synthesis of fluorescent probes. Also, this model scaffold has the ability to further adapt itself in order to acquire different biological and photophysical properties according to desired aims.

Moreover, spectroscopic characterization of the intermediates at each stage and the bioconjugate was evaluated. All fluorescence spectra were obtained for corresponding aqueous solutions. Fluorescence properties of the proposed bioconjugate are representative since the model compound bear the same structure responsible for the photophysical properties. As seen from the fluorescence spectra demonstrated in Figure 1, the bioconjugate exhibits two maximum emissions at 386 nm and 613 nm upon excitation at 350 nm and 555 nm. Compare to the fluorescence characteristics of PIP/anti-CD44 and CF555/anti-CD44, the target bioconjugate revealed a change in fluorescence intensity. Yet but no significant shift in emission wavelength was observed. The results mean that characteristic of structures keep their functions when they join the proposed bioconjugate indicating that anti-CD44 was actually incorporated into the conjugates through the covalent attachment.

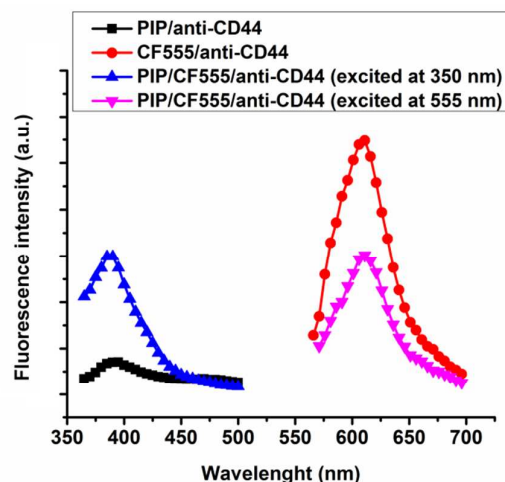


Figure 1. Fluorescence spectra of PIP/anti-CD44, CF555/anti-CD44, and PIP/CF555/anti-CD44 conjugates (excited at 350 and 555 nm).

Atomic force microscopy (AFM) is a powerful tool to observe microscopic surface morphology changes after each successive conjugation. Figure 2 illustrates 3-D and height images (scan area of 2 $\mu\text{m} \times 2 \mu\text{m}$) of the surface of PIP, PIP/anti-CD44 and PIP/CF555/anti-CD44 in tapping mode, respectively.

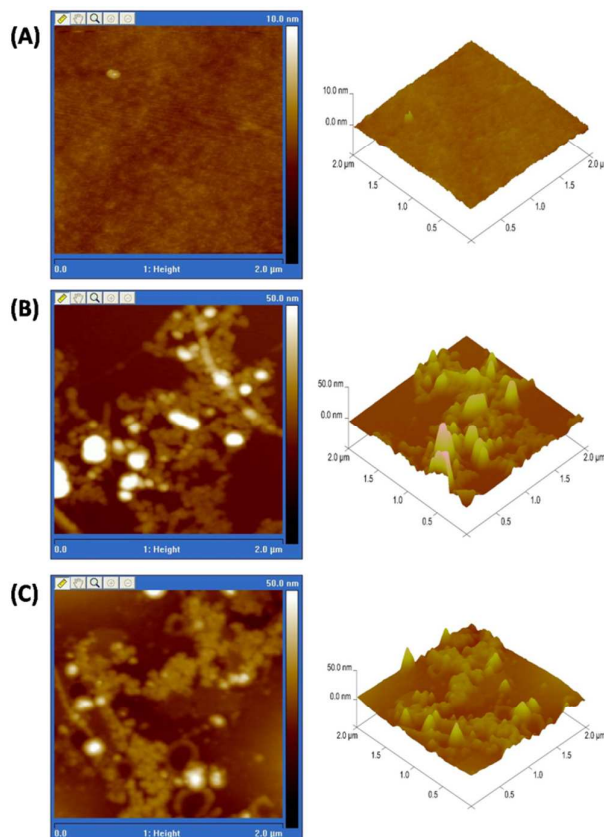


Figure 2. AFM images of PIP (A), PIP/anti-CD44 (B), PIP/CF555/anti-CD44 (C).

To observe microscopy images, plasma oxygen-treated silicon wafer were used as the substrate prior to surface imaging. PIP revealed a homogenous and flat surface (Figure 2A) whereas conjugation of anti-CD44 leads a characteristic hill-valley structure¹⁷ (Figure 2B). The surface undergoes a significant change as a result of bioconjugation process. The dimension was increased by the covalent incorporation of the protein structure with the monomer on the surface. After the proposed probe (PIP/CF555/anti-CD44) was satisfied there was no notably change in surface morphology as expected. Since size of the protein is huge with respect to both PIP and CF555, effect of anti-CD44 was dominant on surface morphology as seen in Figure 2C. The observed change in the dimensions is successfully proven after each stage.

Cytotoxicity

Simple, rapid and sensitive detection of malignant tumours is crucial for the post-treatment of cancer. In this way, many reports and successful diagnosis applications have been demonstrated in the literature.¹⁸⁻²⁰ One of the tumour detection strategies is developing cell imaging agents with functional structures. Moreover, it is important to illuminate and detect cancer cells with a certain and non-invasive way. In the last decade, fluorescent techniques for targeted imaging strategies have gained attraction via using strong fluorescent materials.

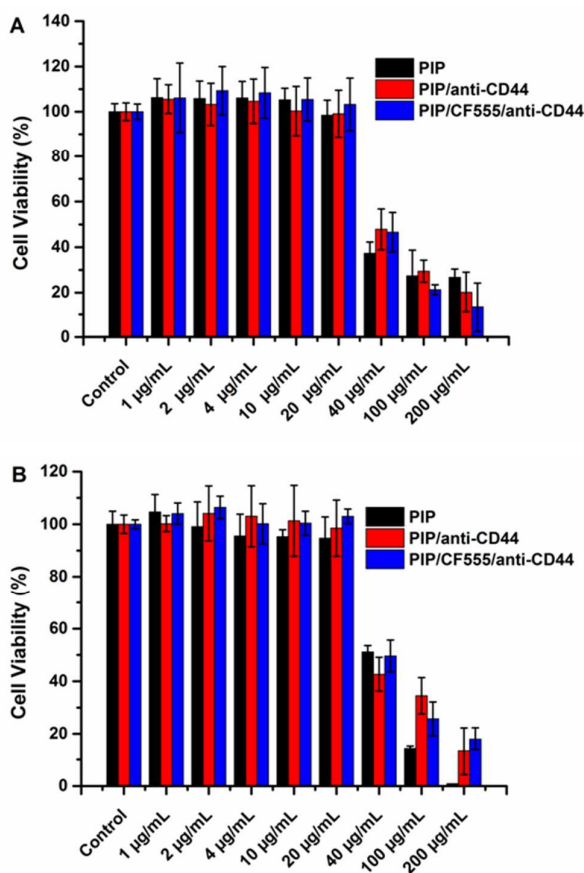


Figure 3. The dose-dependent toxicity of PIP, PIP/anti-CD44 and PIP/anti-CD44 for (A) U87-MG and (B) HaCaT cells. Values are the mean \pm standard deviation of the data ($n = 4$).

CD44 has been characterized as the most common biomolecule and its overexpression was proven for many cancer types such as colon, breast, pancreatic, head and neck cancers.²¹⁻²⁴ Herein, the synthesized bioconjugate bears necessary functional structures and reveals several properties like multicolour fluorescence. It was firstly applied to a CD44 overexpressed U87-MG cells (which was supported by flow analysis) and CD44 negative HaCaT cell line. To create a non-invasive conjugate, it is important to adjust its dose prior to imaging studies. Figure 3A and B demonstrate the effect of PIP monomer, PIP/anti-CD44 and PIP/CF555/anti-CD44 conjugates upon U87-MG and HaCaT keratinocytes in a dose-dependent manner. According to this, the cell survival was decreased to approximately 50 % cell viability after 20 $\mu\text{g/mL}$. As seen in Figures 3A and B, PIP monomer affected the cytotoxicity of cells. In addition, HaCaT cells have shown no viability at the highest concentration of monomer. Since the highest non-toxic dose of monomer and conjugates is 20 $\mu\text{g/mL}$, further studies were carried out with this concentration.

Flow Cytometry

CD44 expression levels of the cell lines were assessed via flow cytometry before targeting studies. Negative control staining with secondary antibody produced similar median fluorescence intensity (MFI); 427 and 359 for HaCaT and U87-MG, respectively (Figure 4A). On the other hand, more than 3-fold increase was seen for U87-MG MFI values after anti-CD44 antibody staining; 2665 and 8794 for HaCaT and U87-MG, respectively (Figure 4B). According to Eq. 1, nMFI was calculated as 3.9, which indicates 4-fold CD44 over expression in U87-MG cells compared to HaCaT cells. These results are in accordance with The Human Protein Atlas25, where 5-fold CD44 over expression is observed in U87-MG cells. As a consequence, U87-MG was used CD44 positive cell line whereas HaCaT was used as control cell line to verify non-specific cell-surface interactions.

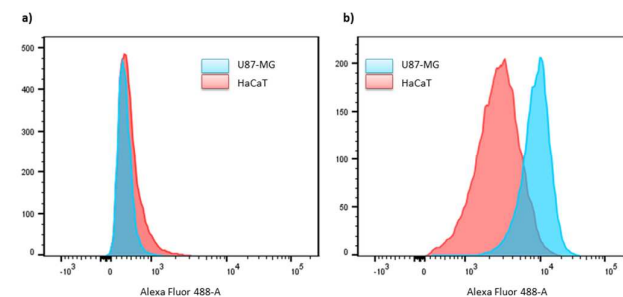


Figure 4. CD44 expressions of U87-MG and HaCaT cell lines. Negative control staining showed no non-specific binding of secondary antibody (A); U87-MG showed higher fluorescence than HaCaT after CD44 staining (B).

Photostability

After the successful synthesis of multi-coloured PIP/CF555/anti-CD44 bioconjugate, both this conjugate and unstained form of conjugate (PIP/anti-CD44) were tested for the photostability. The resultant bioconjugates were diluted as 1:1 with PBS and subsequently portioned. The fluorescence intensities of both unstained conjugate and CF555 dye stained conjugates were recorded in certain time intervals for 30 days by storing the samples at 4°C and dark. All data were only obtained from the emission of the monomer PIP, since the main structure of both conjugates was PIP that excited at 350 nm. The fluorescent measurements demonstrated that no dramatic fluorescent change was observed for PIP/CF555/anti-CD44 for 20 days. However, the fluorescent intensity of unstained PIP/anti-CD44 conjugate increased by 30%.

Cellular Targeting

Fluorescent probes, which are capable of recognizing cancer-associated bio-probes such as receptor proteins and small nucleic acid residues, have great potential for monitoring cancer therapy. In this manner, water-soluble optical probes have been intensely investigated in order to handle non-invasive structures for the relevant cell line.²⁶

Photos of C2 were taken with red filter of fluorescence set up with 100X magnification. All scale bars are 10 µm.

Herein, a newly synthesized PIP monomer which has high hydrophobicity was conjugated with anti-CD44 which was stained with commercial CF555 dye to monitor the CD44 overexpressed cancerous cell lines. In the general concept for the use of CD44 structure, hyaluronic acid (HA) and/or hyaluronan based targeted drug delivery systems, imaging agents have been improved.^{27,28} On the other hand there may be different mechanisms towards the use of HA based targeting strategies since different molecular weight HAs can affect the cell uptake of developed particles in different ways.^{28,29} Beside this, the usage of a monoclonal antibody which has greater specificity to CD44 receptors may open a certain investigation in such studies. Thereby, the developed PIP/CF555/anti-CD44 bioconjugate with multi-coloured optical properties was applied to U87-MG (CD44 positive) and HaCaT keratinocyte (CD44 negative) cells for 2 h. The obtained images from the fluorescence microscopy enabled the most crucial data for this study. Concomitantly, it can be seen that the images belong to CD44 positive cell line U87-MG (Figure 5B, C1 and C2) were brighter than the images of HaCaT cells. Expectedly, the monomer PIP did not play an effective role alone for both cell lines (Figure 5A). Anti-CD44 conjugates seemed to be more internalized into the U87-MG cells compared to HaCaT cells. Furthermore, Figures 5C1 and C2 illustrate the fluorescence of the PIP and CF555 dye, respectively. Hence, it can be claimed that both red and blue fluorescence characters of the bioconjugate showed their properties at the same area in the cells. As seen from the fluorescence images, probe treated U87-MG cells which has overexpressed CD44 receptors, are brighter than the control cell line (HaCaT). There may be an interference of background fluorescence from antibody targeted PIP monomer probe which could not internalize to the cells, effectively. However, there are bright spots in nuclei of U87-MG cells (CD44 positive) which originated from CD44 targeted probe with no background fluorescence. To conclude, it can be understood that the developed multi-coloured probe could be used successfully as an outstanding imaging agent in diagnosis.

Conclusions

The bioconjugated PIP/CF555/anti-CD44 was successfully used as a novel fluorescent bio-probe for targeted imaging of CD44 positive U87-MG cancer cells. The fluorescent bio-probe was designed according to newly proposed approach based on combination of all requirements in one scaffold. The target bioconjugate exhibit both red and blue fluorescence. Also, the generated scaffold facilitated covalent conjugation of the targeting protein anti-CD44 without affecting their photophysical properties. The proposed conjugate was characterized by fluorescence spectroscopy and atomic force microscopy and then tested for *in vitro* studies. Fluorescence images illustrate the cellular internalization of the target bioconjugate in live cells. Flow cytometry studies showed that

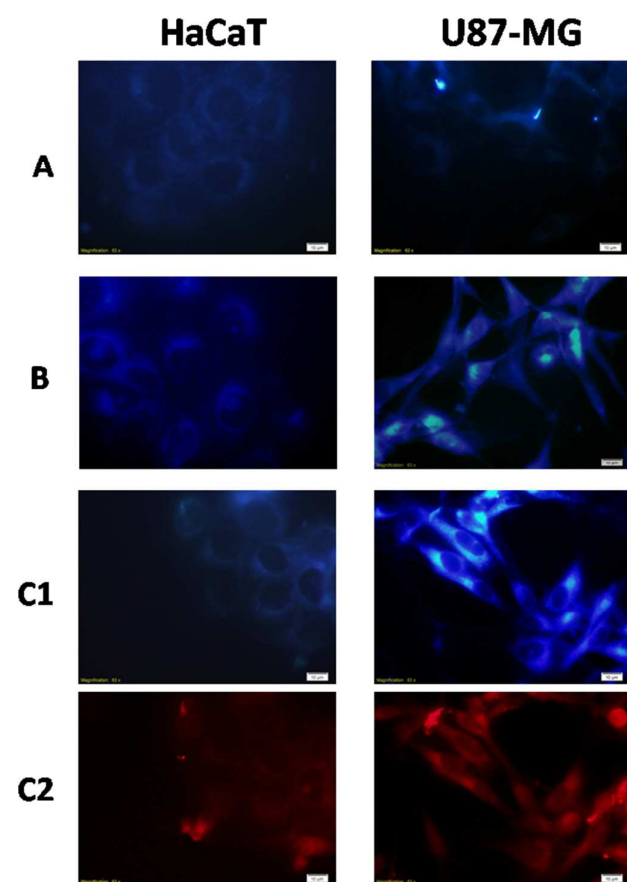
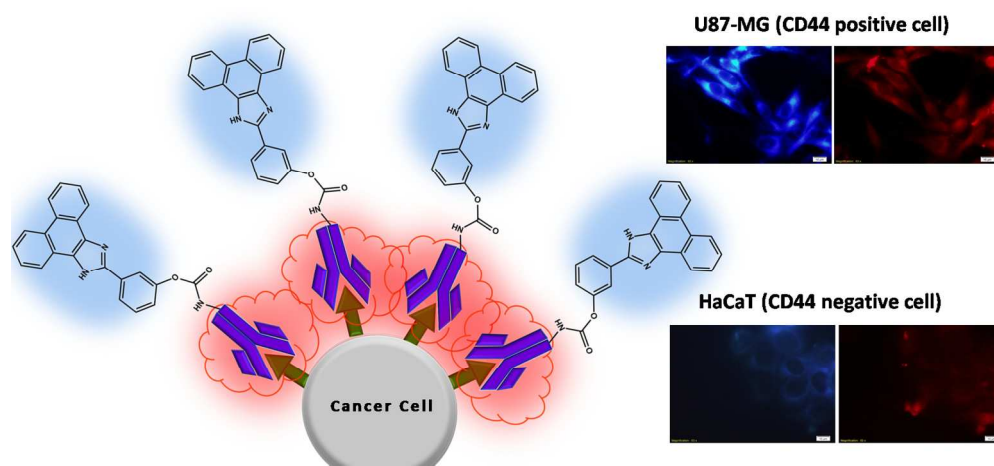


Figure 5. Imaging of HaCaT and U87-MG cells via fluorescence microscopy. Images were obtained after treatment of the cell with PIP monomer (A), PIP/anti-CD44 (B) and PIP/CF555/anti-CD44 (C1 and C2) for 2 h at 37°C and 5.0% CO₂ atmosphere, under humidity. Photos of A, B and C1 were taken with UV filter of fluorescence set up.

U87-MG was used as CD44 positive cell line whereas HaCaT was used as the control cell line. The results present that this strategy to develop such bioconjugate can specifically bind to U87-MG cells with high efficiency. Taking all findings into account, this newly proposed strategy is promising for developing multifunctional probes. Also, such tailor made probes for cellular imaging opens a new viewpoint for further improvement in fluorescence toward *in vitro* and *in vivo* imaging.

Notes and references

- 1 Y. Tsai, C. Hu, C. Chu, Toyoko and Imae, *Biomacromolecules*, 2011, **12**, 4283.
- 2 J. Yao, M. Yang and Y. Duan, *Chem. Rev.*, 2014, **114**, 6130.
- 3 S. Yu, R. Dong, J. Chen, F. Chen, W. Jiang, Y. Zhou, X. Zhu and D. Yan, *Biomacromolecules*, 2014, **15**, 1828.
- 4 A. Duarte, K.Y. Pu, B. Liu and G.C. Bazan, *Chem. Mater.*, 2011, **23**, 501.
- 5 S. Md. Sharker, S. M. Kim, S. H. Kim, I. In, H. Lee and S.Y. Park, *J. Mater. Chem. B*, 2015, **3**, 5833.
- 6 G. Unak, F. Ozkaya, E.İ. Medine, O. Kozgus, S. Sakarya, R. Bekis, P. Unak and S. Timur, *Colloids Surf. B*, 2012, **90**, 217.
- 7 R. Bongartz, D. Ağ, M. Selecı, J. Walter, E.E. Yalcinkaya, D.O. Demirkol, F. Stahl, S. Timur and T. Scheper, *J. Mater. Chem. B*, 2013, **1**, 522.
- 8 D. Ag, M. Selecı, R. Bongartz, M. Can, S. Yurteri, I. Cianga, F. Stahl, S. Timur, T. Scheper and Y. Yagci, *Biomacromolecules*, 2013, **14**, 3532.
- 9 J. Shen, K. Li, L. Cheng, Z. Liu, S. Lee and J. Liu, *ACS Appl. Mater. Interfaces*, 2014, **6**, 6443.
- 10 S. Bera, M. Ghosh, M. Pal, N. Das, S. Saha, S.K. Dutta and S. Jana, *RSC Adv.*, 2014, **4**, 37479.
- 11 E.İ. Medine, D. Odacı, B.N. Gacal, S. Sakarya, P. Unak, S. Timur and Y. Yagci, *Macromol. Biosci.*, 2010, **10**, 657.
- 12 D.G. Colak, I. Cianga, D.O. Demirkol, O. Kozgus, E.İ. Medine, S. Sakarya, P. Unak, S. Timur and Y. Yagci, *J. Mater. Chem.*, 2012, **22**, 9293.
- 13 L. Feng, L. Liu, F. Lv, G.C. Bazan and S. Wang, *Adv. Mater.*, 2014, **26**, 3926.
- 14 M. Akin, R. Bongartz, J.G. Walter, D.O. Demirkol, F. Stahl, S. Timur and T. Scheper, *J. Mater. Chem.*, 2012, **22**, 11529.
- 15 G.T. Hermanson, *Bioconjugate Techniques*, 2nd ed, Elsevier Academic Press: San Diego, CA, 2004; p 196.
- 16 D. Ag, R. Bongartz, L.E. Dogan, M. Selecı, J. Walter, D.O. Demirkol, F. Stahl, S. Ozcelik, S. Timur and T. Scheper, *Colloids Surf. B*, 2014, **114**, 96.
- 17 H.S. Seo, Y.M. Ko, J.W. Shim, Y.K. Lim, J. Kook, D. Cho and B.H. Kim, *Appl. Surf. Sci.*, 2010, **257**, 596.
- 18 M. Yuksel, D.G. Colak, M. Akin, I. Cianga, M. Kukut, E.İ. Medine, M. Can, S. Sakarya, P. Unak, S. Timur and Y. Yagci, *Biomacromolecules*, 2012, **13**, 2680.
- 19 F. Ekiz Kanik, D. Ag, M. Selecı, M. Kesik, H. Akpınar, G. Hizalan, F.B. Barlas, S. Timur and L. Toppare, *Biotechnol. Prog.*, 2014, **30**, 952.
- 20 M. Liu, J. Ji, X. Zhang, X. Zhang, B. Yang, F. Deng, Z. Li, K. Wang, Y. Yang and Y. Wei, *J. Mater. Chem. B*, 2015, **3**, 3476.
- 21 M. Al-Hajj, M.S. Wicha, A. Benito-Hernandez, S.J. Morrison and M.F. Clarke, *Proc. Natl. Acad. Sci. U. S. A.*, 2003, **100**, 3983.
- 22 A.T. Collins, P.A. Berry, C. Hyde, M.J. Stower and N. J. Maitland, *Cancer Res.*, 2005, **65**, 10946.
- 23 P. Dalerba, S.J. Dylla, I.K. Park, R. Liu, X. Wang, R.W. Cho, T. Hoey, A. Gurney, E.H. Huang, D.M. Simeone, A.A. Shelton, G. Parmiani, C. Castelli and M.F. Clarke, *Proc. Natl. Acad. Sci. U. S. A.*, 2007, **104**, 10158.
- 24 C. Li, D.G. Heidt, P. Dalerba, C.F. Burant, L. Zhang, V. Adsay, M. Wicha, M.F. Clarke and D.M. Simeone, *Cancer Res.*, 2007, **67**, 1030.
- 25 M. Uhlen, L. Fagerberg, B. M. Hallström, C. Lindskog, P. Oksvold, A. Mardinoglu, A. Sivertsson, C. Kampf, E. Sjöstedt, A. Asplund, I. Olsson, K. Edlund, E. Lundberg, S. Navani, C. A. Szgyarto, J. Odeberg, D. Djureinovic, J. O. Takanen, S. Hober, T. Alm, P. H. Edqvist, H. Berling, H. Tegel, J. Mulder, J. Rockberg, P. Nilsson, J. M. Schwenk, M. Hamsten, K. von Feilitzen, M. Forsberg, L. Persson, F. Johansson, M. Zwahlen, G. von Heijne, J. Nielsen and F. Pontén, *Science*, 2015, **347**, 1260419.
- 26 X. Xu, H. Cheng, W. Chen, S. Cheng, R. Zhuo and X. Zhang, *Sci. Rep.*, 2013, **3**, Article number: 2679, doi:10.1038/srep02679.
- 27 S.R. Hamilton, S.F. Fard, F.F. Paiwand, C. Tolg, M. Veiseh, C. Wang, J.B. McCarthy, M.J. Bissell, J. Koropatnick and E.A. Turley, *J. Biol. Chem.*, 2007, **282**, 16667.
- 28 H.S. ShaQhattal and X. Liu, *Mol. Pharmacol.*, 2011, **8**, 1233.
- 29 M.H. El-Dakdouki, D.C. Zhu, K. El-Boubbou, M. Kamat, J. Chen, W. Li and X. Huang, *Biomacromolecules*, 2012, **13**, 1144.



450x219mm (96 x 96 DPI)